 CMES, vol.116, no.3, pp.391-406, 2018

UPFC Based Real-Time Optimization of Power Systems for Dynamic Voltage Regulation

Serhat Berat Efe[1, *]

Abstract: Flexible alternating current transmission system (FACTS) components are used to utilize the electrical transmission lines at their optimum capacity. The best way to achieve this optimization is to manage the active and reactive power flows. A unified power flow controller (UPFC) is one of the most significant devices developed for the effective control of power flows. Although conventional UPFC structures can be used to achieve this process, the expansion of power systems has led to the necessity of developing various UPFC devices. This paper focuses on an advanced real time control approach of UPFC for dynamic voltage regulation. The developed model is incorporated in the Gauss-Seidel (GS) power flow algorithm and the proposed method is validated on the IEEE-30 bus system that is designed under MATLAB/Simulink platform. As the proposed method was validated by comparing with the normal operating conditions, advantages were observed on two cases. In the first case, a generator outage is applied to system to observe behavior of proposed model in power loss conditions. In the second case, line fault conditions were used for observation. The results from testing the model for both cases prove that the approach has positive effects on dynamic power systems.

Keywords: Power flow control, UPFC, FACTS devices, power system analysis computing, Gauss-Seidel algorithm.

1 Introduction

Energy efficiency is one of the most important issues for modern power systems. Besides various applications, FACTS devices have been widely used for such research since they were first introduced in the late 1980s. IEEE defines FACTS as “a power-electronic based system and other static equipment that provide control of one or more AC-transmission system parameters to enhance controllability and increase power-transfer capability” [Hingorani and Gyugyi (2000)]. These devices are used to increase the power transfer capacity, regulating the voltage amplitude and reducing power losses of electrical networks and enhance the ability of controlling such systems [Shojaeian, Naeeni, Dolatshahi et al. (2014)]. The most common FACTS devices used in application and research are the static synchronous compensator (STATCOM), static series synchronous compensator (SSSC), static var compensator (SVC), thyristor controlled series capacitor (TCSC), and UPFC.

[1] Bitlis Eren University, Department of Electrical and Electronics Engineering, Bitlis, 13000, Turkey.

[*] Corresponding Author: Serhat Berat Efe. Email: sbefe@beu.edu.tr.

A UPFC is the combination of a STATCOM and a SSSC that are coupled via a DC link to allow the bidirectional flow of active power between the series output terminals of the SSSC and the shunt output terminals of the STATCOM and can be defined as the most powerful FACTS device [Morsli, Tayeb, Mouloud et al. (2012); Banaei and Kami (2010)]. Thus, a UPFC is capable of directing real and reactive power flows through a desired route and regulating the system voltage by reactive power compensation [Gyugyi, Schauder, Williams et al. (1995)]. A UPFC is a multi-functional controller that can simultaneously control all the parameters of the system: The line impedance, the transmission angle, and bus voltage [Yuan, de Haan, Ferreira et al. (2010)], which also improves the power flows [Cárdenasa (2014); Kamel and Jurado (2014)]. In addition, UPFC is effective for achieving power flow redistribution of the transmission system [Shao and Vittal (2006); Rajabi, Fotuhi and Othman (2015); Shaheen, Rashed and Cheng (2011); Kim, Lim and Moon (2000)]. The configuration of a UPFC is based on the concept of voltage source converter (VSC) [Kamel, Juradoa and Pecas (2015)]. In general terms, FACTS devices, especially the UPFC, have become a fundamental necessity for power flow control algorithms in the planning, operation and control stages.

There are comprehensive studies on power flow control using a UPFC. In Yadav et al. [Yadav and Soni (2016)], the UPFC is located at the sending end of system for line power flow optimization. Researchers have developed an algorithm for determining a UPFC location to enhance the power system capacity in Taher et al. [Taher and Amooshahi (2012)]. Since UPFC modelling is difficult to investigate a power injection method based steady state UPFC model was designed in Wang et al. [Wang, Song, Yan et al. (2011)], and a dynamic model was developed for active power regulation in Ahmad et al. [Ahmad, Albatsh, Mekhilef et al. (2014)]. Proposed study differs from literature with its online control capability. Literature review shows that whether there were studies on power flow analysis in ill-conditioned systems [Ghatak and Mukherjee (2017); Farag, El-Saadany, El Shatshat et al. (2011); Pourbagher and Derakhshandeh (2018)], they were for steady state conditions in general. In addition, power flow analysis methods are formulated by incorporating necessary modifications in Newton Raphson [Zhang and Chen (1997); Da Costa, Martins and Pereira (1999)], Gauss Seidel [Teng (2002)] and other existing methods [Garcia, Pereira, Carneiro et al. (2000)], obtained results were not used directly for regulation. As there were also studies on converter controlling [Thiyagarajan and Somasundaram (2017)], using the power flow analysis results to control the converters to regulate system values is the major advantage of proposed method.

The motivation for this study was the regulation of busbar voltages of power systems during both steady state and transient conditions. In keeping with this aim, the remainder of the paper is organized as follows; Section 2 presents the proposed structure and development of the algorithm, Section 3 details the developed model, Section 4 describes the validation of the model using dynamic power system cases, and finally in Section 5, the results are discussed using the obtained data.

2 Materials and methods

The equivalent circuit of a conventional UPFC is shown in Fig. 1.

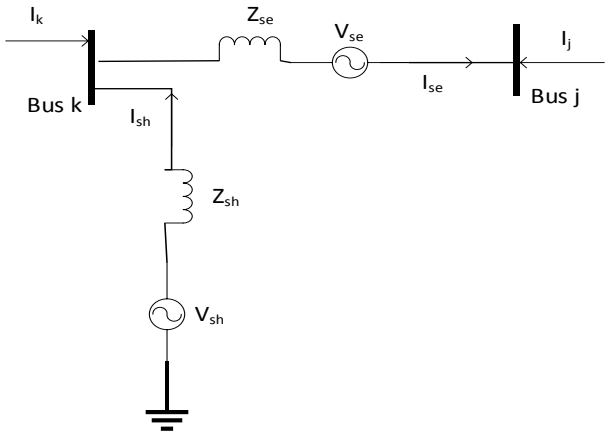

Figure 1: Equivalent circuit of the UPFC

The ideal voltage sources for the UPFC, which are shown as V_{sh} and V_{se} in Fig. 1, can be described as:

$$\underline{V}_{sh} = V_{sh}(\cos\theta_{sh} + j\sin\theta_{sh}) \tag{1}$$

$$\underline{V}_{se} = V_{se}(\cos\theta_{se} + j\sin\theta_{se}) \tag{2}$$

The basic schematic diagram of the proposed UPFC is given in Fig. 2. This structure is a developed version of conventional UPFC, which is consist of series and shunt transformers and two converters that connected via DC link, by adding a data processing unit (DPU).

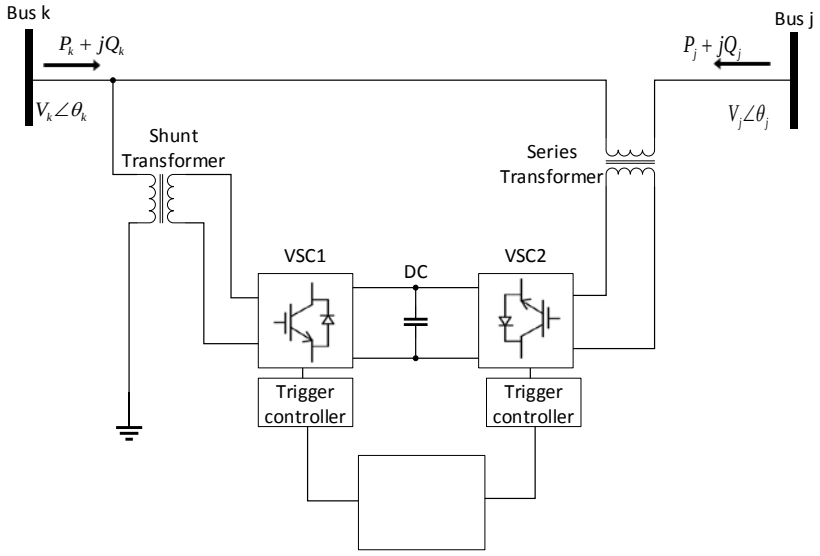

Figure 2: Basic schematic diagram of the UPFC

DPU is the most important section of proposed method. In this unit, obtained data is processed and triggering angles are determined. These values are transmitted to trigger controllers of both converters and output values of VSC1 and VSC2 are controlled.

The main functions of the UPFC elements need to be defined to attain a detailed understanding of whole structure. The converters, which are classified as series and shunt, change the DC voltage to a pure AC signal with a pre-defined magnitude and frequency with the phase shift according to the reference phase. The series converter controls the active and reactive power flows on the transmission line by inserting a voltage with controlled magnitude and phase angle via a series transformer. Based on this process, the parallel branch takes the injected real power from the system and transmits it to a series branch over a DC link. The DC link capacitor is designed to provide a real power exchange between the series and shunt converters and provide an appropriate DC voltage to control the internally circulated reactive power. This makes the UPFC an ideal AC-AC converter.

The active and reactive power values at each busbar can be obtained mathematically from the following power flow equations for the UPFC circuit given in Fig. 2;

$$P_k = |V_k| |V_j| \sum_{i=1}^{N} \left(G_{kj} \cos \delta_{kj} + B_{kj} \sin \delta_{kj} \right) \tag{3}$$

$$Q_k = |V_k| |V_j| \sum_{i=1}^{N} \left(G_{kj} \cos \delta_{kj} - B_{kj} \sin \delta_{kj} \right) \tag{4}$$

where V_k and V_j are voltages of the *k* and *j* buses, respectively, *N* is the number of system buses, G_{kj} is conductance, B_{kj} is susceptance, and δ_{kj} is the angle between the *k* and *j* buses.

According to the aim of this study, voltage stability, which is the main factor of dynamic stability, can be expressed as;

$$\Delta V_i = \frac{1}{\sqrt{p}} \sqrt{\sum_{i=1}^{p} \left(V_i \right)^2} \tag{5}$$

while

$$V_i = V_{slc} - \sum_{i=1}^{n} Z_i \left(\frac{P_i - jQ_i}{V_i} \right) \tag{6}$$

In Eqs. (5) and (6), ΔV_i is the voltage stability indicator, V_i is the bus voltage, V_{slc} is the voltage of slack bus, Z_i is the impedance of the ith bus, P_i and Q_i are the active and reactive power values of bus *i*, respectively, where i=1, 2, 3,…, n.

2.1 The Gauss-Seidel power flow analysis method

The proposed algorithm is based on the Gauss-Seidel power flow analysis method because of its valuable advantages in that it not only shares the Jacobi Method simplicity of programming for computer-based analysis, but also offers the additional benefit of improved convergence performance. The Jacobi Method calculates the new values for all the busbar voltages before replacing the old values of voltages with the new calculation,

and the Gauss-Seidel Method uses each busbar voltage immediately after it is calculated [Powell (2004)]. Therefore, this calculation leads to an improved convergence. In the Gauss-Seidel Method, the computation time per iteration is less according to other algorithms, and it has linear convergence characteristics. The algorithm duration is vital for dynamic systems, and this is the most important reason why this method was selected for the proposed study; however, the choice of slack bus is critical to achieve the best convergence.

The Gauss-Seidel power flow analysis is an iterative method; thus, it is necessary to define the elements of this structure. According to this requirement, the following equations are formed. The voltage at the k^{th} bus can be denoted by;

$$V_k = |V_k| \angle \delta_k = |V_k| \left(\cos \delta_k + j \sin \delta_k \right) \tag{7}$$

also, the self-admittance of bus *k* as;

$$Y_{kk} = |Y_{kk}| \angle \theta_{kk} = |Y_{kk}| \left(\cos \theta_{kk} + j \sin \theta_{kk} \right) = G_{kk} + jB_{kk} \tag{8}$$

and the admittance between the *k* and *j* buses can be given as;

$$Y_{kj} = |Y_{kj}| \angle \theta_{kj} = |Y_{kj}| \left(\cos \theta_{kj} + j \sin \theta_{kj} \right) = G_{kj} + jB_{kj} \tag{9}$$

A conventional power system consists of *n* buses. Therefore, the current injected at bus *k* for a power system that contains a total number of n buses can be given as;

$$I_k = Y_{k1}V_1 + Y_{k2}V_2 + \cdots + Y_{kn}V_n = \sum_{i=1}^{n} Y_{ki}V_i \tag{10}$$

Therefore, the complex power at bus *k* can be given by;

$$P_k - jQ_k = V_k^* I_k = V_k^* \sum_{i=1}^{n} Y_{ki}V_i$$

$$= \sum_{i=1}^{n} |Y_{ki}V_kV_i| \left(\cos \delta_k - j \sin \delta_k \right) \left(\cos \theta_{ki} + j \sin \theta_{ki} \right) \left(\cos \delta_i + j \sin \delta_i \right) \tag{11}$$

Finally, by applying the trigonometrical conversions to (11), the real and reactive power equations can be obtained as;

$$P_k = \sum_{i=1}^{n} |Y_{ki}V_kV_i| \cos \left(\theta_{ki} + \delta_i - \delta_k \right) \tag{12}$$

$$Q_k = -\sum_{i=1}^{n} |Y_{ki}V_kV_i| \sin \left(\theta_{ki} + \delta_i - \delta_k \right) \tag{13}$$

The actual power system busbars both generate and consume active and reactive powers. According to this fact and for the most reliable convergence, the net active and reactive powers must be used for power flow analysis. Therefore, it is necessary to calculate the net power values for all busbars.

If the P_{Gk} and Q_{Gk} are the generated active and reactive powers, P_{Ck} and Q_{Ck} are the consumed active and reactive powers for bus *k*, respectively, then the net power values for bus *k* are;

$$P_{k,net} = P_{Gk} - P_{Ck} \tag{14}$$

$$Q_{k,net} = Q_{Gk} - Q_{Ck} \tag{15}$$

Using the new formulation, the complex power equation given in Eq. (7) can be written as

$$P_{k,net} - jQ_{k,net} = V_k^* \sum_{i=1}^{n} Y_{ki} V_i = V_k^* \left[Y_{k1} V_1 + Y_{k2} V_2 + \cdots + Y_{kk} V_k + \cdots + Y_{kn} V_n \right] \tag{16}$$

Also, to obtain the voltage of the such busbar,

$$V_k = \frac{1}{Y_{kk}} \left[\frac{P_{k,net} - jQ_{k,net}}{V_k^*} - Y_{k1} V_1 - Y_{k2} V_2 - \cdots - Y_{kn} V_n \right] \tag{17}$$

The net active and reactive power values can be calculated separately as;

$$P_{k,net} = \Re e \left[V_k^* \sum_{i=1}^{n} Y_{ki} V_i \right] = \Re e \left[V_k^* \left\{ Y_{k1} V_1 + Y_{k2} V_2 + \cdots + Y_{kk} V_k + \cdots + Y_{kn} V_n \right\} \right] \tag{18}$$

$$Q_{k,net} = -\operatorname{Im} \left[V_k^* \sum_{i=1}^{n} Y_{ki} V_i \right] = -\operatorname{Im} \left[V_k^* \left\{ Y_{k1} V_1 + Y_{k2} V_2 + \cdots + Y_{kk} V_k + \cdots + Y_{kn} V_n \right\} \right] \tag{19}$$

hence for the t^{th} iteration,

$$P_{k,net}^{(t)} = \Re \left[V_k^{*(t-1)} \left\{ Y_{k1} V_1 + Y_{k2} V_2^{(t)} + \cdots + Y_{kk} V_k^{(t-1)} + \cdots + Y_{kn} V_n^{(t-1)} \right\} \right] \tag{20}$$

$$Q_{k,net}^{(t)} = -\operatorname{Im} \left[V_k^{*(t-1)} \left\{ Y_{k1} V_1 + Y_{k2} V_2^{(t)} + \cdots + Y_{kk} V_k^{(t-1)} + \cdots + Y_{kn} V_n^{(t-1)} \right\} \right] \tag{21}$$

Iteration number of the calculation is determined by the pre-set convergence value. While the system convergences, net active and reactive power data is sent to output. In addition, to avoid infinite loop, iteration number can be limited before starting the algorithm.

3 Architecture of the proposed controller

In the proposed method, the designed UPFC consists of two main units. One of the units, which can be described as hardware, is used to collect the necessary data from the system. This structure was designed using MATLAB/Simulink. The second and the main unit is the code-based structure of the controller, which includes the power flow algorithm. As the basis of the study, the algorithm was created using the MATLAB editor to enhance the power capability and regulate the system parameters. The proposed algorithm is divided into two main sections; data preparation and the Gauss-Seidel power flow algorithm. These programs are based on Eqs. (7)-(21) given above. A timer sub-program

is embedded into the algorithm, which allows the power flow analysis to be repeated to observe the whole system by pre-set period.

The system block structure is shown in Fig. 3, and the internal structure of controller is given in Fig. 4.

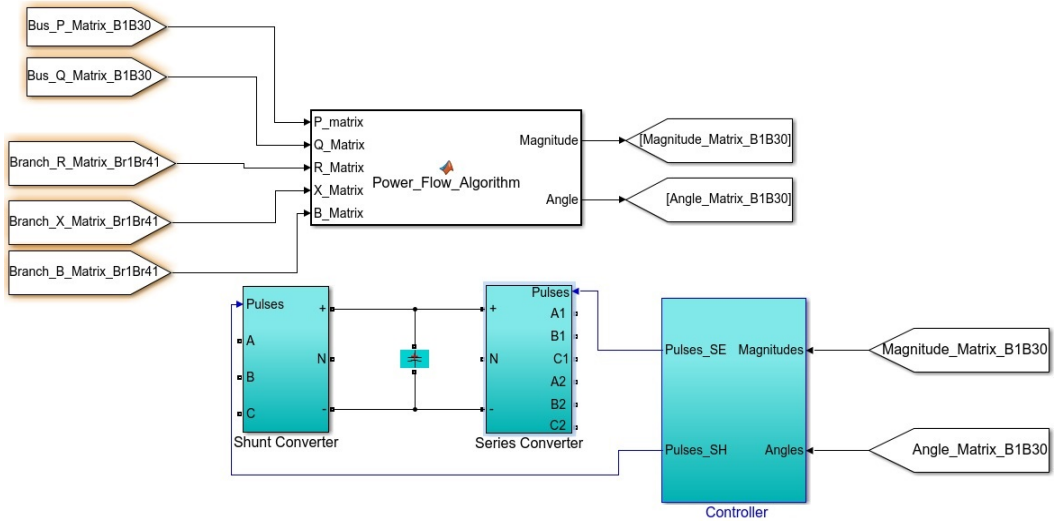

Figure 3: Proposed system structure

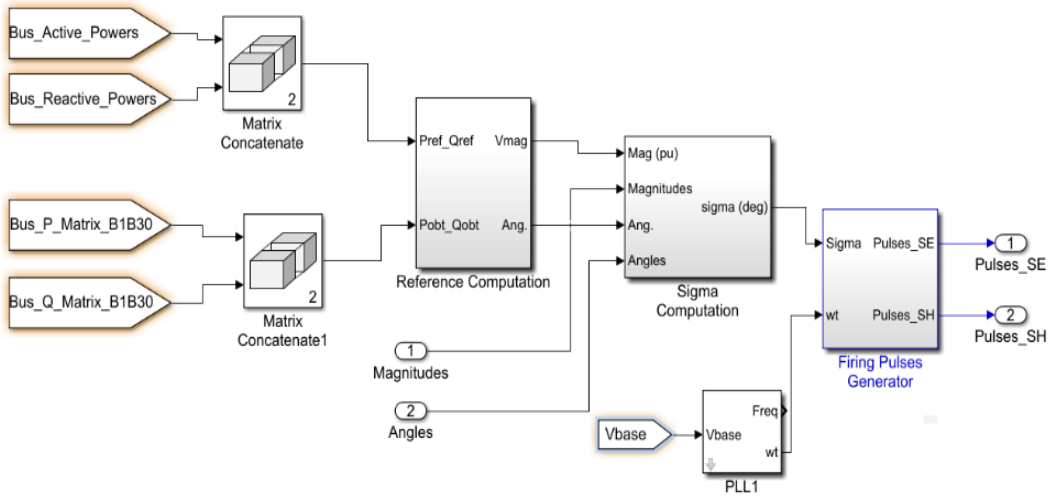

Figure 4: Internal structure of controller

The controller was designed to determine and adjust pulses for series and shunt converters. The active-reactive power values and branch data were collected and used in the power flow algorithm presented in Fig. 3. Voltage amplitude and angle values were the output of this algorithm. Algorithm output data were sent to the controller in matrix form. In addition, the instantaneous power values were supplied to controller. These were compared with the reference values, which constituted the normal operation data for this

study. This comparison was performed via the reference computation block shown in Fig. 4. Reference computation block calculates the reference magnitudes and angles. Sigma computation block was used to determine the sigma value for the pulse generator by comparing algorithm output data and calculated reference values. Finally, the trigger timing of the pulses was determined and used for controlling of series and shunt converters.

4 Dynamic voltage regulation

Developed model is implemented in MATLAB/Simulink platform via a computer with 16 GB RAM and Intel Core i7 processor. The proposed method was tested in three cases. In the first case, the standard IEEE-30 bus system was used for testing. This case was utilized to compare the results of the proposed algorithm using pre-known values for validation. The results of the power flow analysis for the IEEE-30 bus system [Zimmerman, Murillo-Sanchez and Thomas (2011)] were compared with the results of the proposed method for validation in the current study. As the performance of the algorithm can be precisely observed on a dynamic system that contains nonlinear changes, such a bus system can be modified by changing the power values. Based on this method, for the second case, the system was modified by disconnecting a generator unit of one bus, and the results were noted. In the third case, a line fault was applied to the system to determine the advantages of the proposed method.

4.1 Case 1-standard IEEE-30 bus system

Power flow analysis was performed for the IEEE-30 bus system at steady state operation as given in Christie [Christie (1993)], and the results were compared with the proposed method for validation. The UPFC is located on the highest power-losing branch of the IEEE-30 bus system between buses 1 and 2 (branch 1) as shown in Fig. 5.

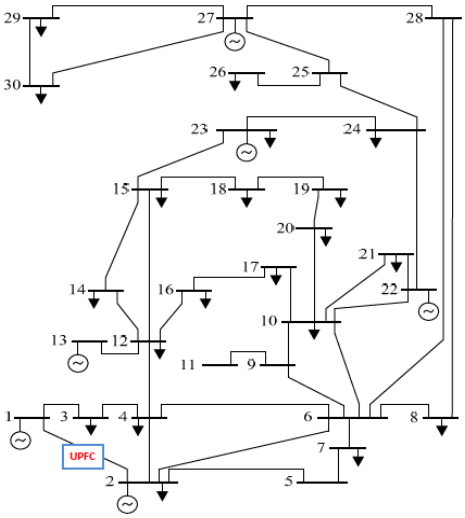

Figure 5: IEEE-30 bus system one line diagram with the UPFC

For system validation, the voltage magnitude and angle values of the proposed structure were compared with the results of the conventional power flow analysis algorithm, which are given in Tab. 1. The magnitude values are in terms of pu, where the base apparent power is 100 MVA.

Table 1: Comparison results for validation

	Voltage Amplitude (pu)		Angle (deg.)	
Bus No.	Conventional	Proposed	Conventional	Proposed
1	1.06	1.0600	0	0
2	1.045	1.0441	-5.378	-5.352
3	1.021	1.0207	-7.529	-7.532
4	1.012	1.0118	-9.279	-9.282
5	1.01	1.0100	-14.149	-14.162
6	1.011	1.0103	-11.055	-11.062
7	1.003	1.0024	-12.852	-12.862
8	1.01	1.0100	-11.797	-11.812
9	1.051	1.0509	-14.098	-14.112
10	1.045	1.0451	-15.688	-15.702
11	1.082	1.0820	-14.098	-14.112
12	1.057	1.0571	-14.933	-14.942
13	1.071	1.0710	-14.933	-14.942
14	1.043	1.0423	-15.825	-15.832
15	1.038	1.0377	-15.916	-15.932
16	1.045	1.0444	-15.515	-15.522
17	1.04	1.0399	-15.85	-15.862
18	1.028	1.0282	-16.53	-16.542
19	1.026	1.0257	-16.704	-16.712
20	1.03	1.0297	-16.507	-16.522
21	1.033	1.0327	-16.131	-16.142
22	1.034	1.0333	-16.116	-16.132
23	1.027	1.0272	-16.307	-16.322
24	1.022	1.0216	-16.483	-16.492
25	1.018	1.0173	-16.055	-16.072
26	1.000	0.9997	-16.474	-16.482
27	1.024	1.0232	-15.53	-15.542
28	1.007	1.0068	-11.677	-11.692
29	1.004	1.0034	-16.759	-16.772
30	0.992	0.9919	-17.642	-17.652

The busbar angle values are the difference of the angles of busbars with the slack busbar. For the static system, the actual value of the voltage angle of the slack busbar was 98.432°. As a result, the angle value of busbar one, the slack busbar, was zero. According to the comparisons shown in Tab. 1, the proposed model was validated since there were approximately the same values as achieved by the iterative method, which was based on the Newton-Raphson method. This proves that proposed system is appropriate for use in power flow studies.

4.2 Case 2-generator outage

The investigation of the static system to observe the effect of the proposed UPFC structure on a dynamic system revealed that the IEEE-30 system was modified by an outage, which was expected to occur at the generator of bus 2. The major advantages and the regulating performance of the proposed system can be observed in this case.

The simulation was performed to determine the effects of the proposed method on the system. Line current values were limited to 110% of nominal for safety and protection. According to such a limitation, the regulating performance of proposed method was also limited and could not restore the amplitude values exactly to the pre-fault status. Therefore, a difference occurred in comparison with steady state operating conditions.

For the simulation, the algorithm repeating time was set to 1 second in the timer sub-program. There were two main points that validated the proposed model. At the 1.8th second, generator 2 outage was applied to the bus, and this caused a decrement in the voltage amplitude. This value decreased to 1.0163 pu in the normal system. As the timer subprogram was adjusted to perform power flow analysis per second, it was activated at the 2nd second, and the busbar amplitude improved to 1.0383 pu. At the 3.8th second, the generator was reactivated to its original situation, and effects were observed. Fig. 6 presents the steady state value and the system response with and without UPFC, showing that the proposed control algorithm was successful in returning the voltage amplitude to the target value in a short period, but had no effect in the case of the system returning to normal operating conditions.

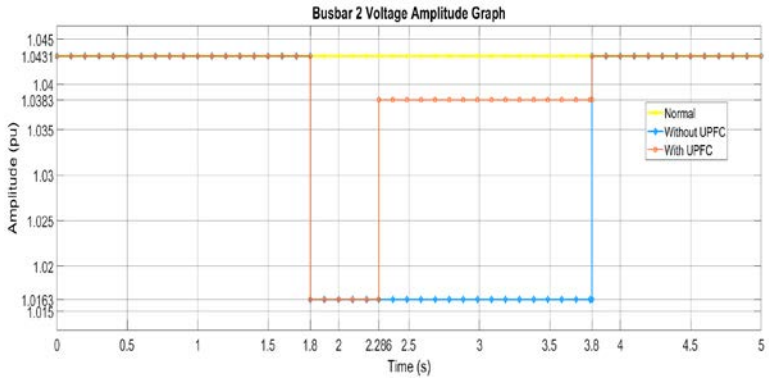

Figure 6: Busbar 2 voltage amplitude variation

The system convergence was set to 10^{-5} to obtain the most stable results. As speed is one of the most important issues in real-time optimization, it is necessary to determine the

number of iterations together with duration for convergence. It took 0.286 seconds for 34 iterations in the current case.

The proposed algorithm regulates the power flow analysis parameters by comparing them with the preset values. The average voltage amplitudes during the nonlinear condition for other buses of the IEEE-30 bus system are summarized in Tab. 2.

Table 2: Results for the other buses

	Average Voltage Amplitudes (pu)			
Bus No.	Normal Operating	Without UPFC	With Proposed Method	Difference
1	1.0600	1.0600	1.0600	0.0000
3	1.0207	1.0088	1.0192	0.0104
4	1.0118	0.9974	1.0086	0.0112
5	1.0100	0.9913	1.0026	0.0113
6	1.0103	0.9952	1.0076	0.0124
7	1.0024	0.9857	0.9998	0.0141
8	1.0100	0.9960	1.0025	0.0065
9	1.0509	1.0423	1.0494	0.0071
10	1.0451	1.0355	1.0396	0.0041
11	1.0820	1.0820	1.0820	0.0000
12	1.0571	1.0504	1.0559	0.0055
13	1.0710	1.0710	1.0710	0.0000
14	1.0423	1.0350	1.0401	0.0051
15	1.0377	1.0299	1.0343	0.0044
16	1.0444	1.0363	1.0398	0.0035
17	1.0399	1.0307	1.0386	0.0079
18	1.0282	1.0196	1.0260	0.0064
19	1.0257	1.0167	1.0230	0.0063
20	1.0297	1.0206	1.0271	0.0065
21	1.0327	1.0229	1.0300	0.0071
22	1.0333	1.0234	1.0310	0.0076
23	1.0272	1.0183	1.0256	0.0073
24	1.0216	1.0113	1.0192	0.0079
25	1.0173	1.0049	1.0140	0.0091
26	0.9997	0.9870	0.9943	0.0073
27	1.0232	1.0097	1.0211	0.0114
28	1.0068	0.9922	1.0022	0.0100
29	1.0034	0.9895	1.0002	0.0107
30	0.9919	0.9779	0.9898	0.0119

Significant inferences can be drawn according to the results in Tab. 2. The load only buses (3, 4, 7, 8, 10, 12, 14, 15, 16, 17, 18, 19, 20, 21, 24, 26, 29, 30) were more affected by outage than the others. On the other hand, the busbars with generators (1, 13, 22, 23, 27) showed less reaction. It is clear from the results that the value of influence increased relatively as the distance of the busbar increased from the connection point of the UPFC.

4.3 Case 3-line fault

Power system faults, which can be considered as stochastic, affect the reliability, security, and quality of supplied energy of the system. Different events, such as lightning, and insulation breakdown are common causes of overhead power system faults. Since the proposed method is designed to manage busbar voltages for transient conditions, system performance for such conditions is discussed in this case. A line fault is supposed to occur at line 14, which is between busbars 9 and 10. It is vital to intervene in the power system as quickly as possible in fault conditions in terms of safety and stability. Thus, the timer subprogram was adjusted to 0.5 seconds for a more sensitive observation and control. It took 214 milliseconds for 29 iterations to reach convergence for line fault conditions. The convergence graphs for cases 2 and 3 are given in Fig. 7.

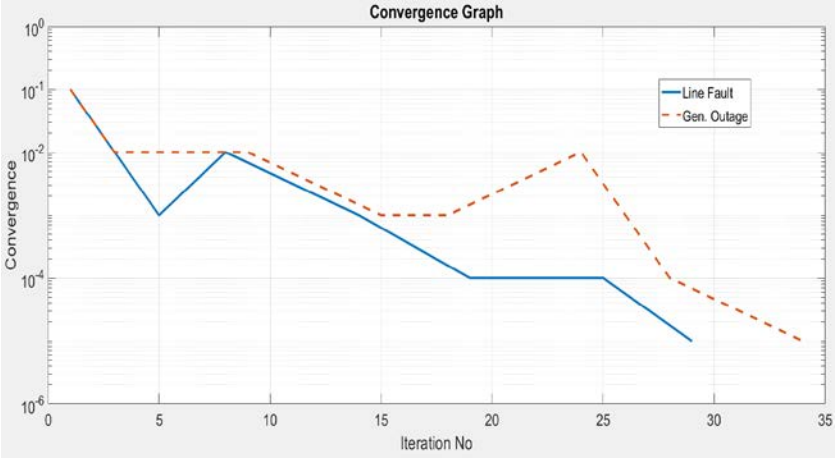

Figure 7: Convergence graph for both cases

The comparison of the system results with and without the developed method is given in Tab. 3.

In this case, the most significant result was the increment of amplitude value of bus 9 during line fault to 1.0572 pu, where it had a value of 1.0509 pu in normal conditions. This reveals another advantage of the proposed method since it not only increased the busbar voltages, but was also able to decrease them for stability if necessary.

These results were obtained for the safe operating conditions of system. In addition, the transmission line loading values were observed for the case. As an example, the comparison of normal operating conditions during nonlinear conditions without UPFC and with the proposed model loading values for some lines in terms of ampere percentage is given together in Tab. 4 to provide a clear understanding. It should be noted that the lines between buses 4-12, 6-9 and 6-10 included transformer units.

Table 3: Line fault results

	Average Voltage Amplitudes (pu)			
Bus No.	Normal Operating	Without UPFC	With Proposed Method	Difference
1	1.0600	1.0600	1.0600	0.0000
2	1.0431	1.0427	1.0430	0.0003
3	1.0207	1.0188	1.0206	0.0018
4	1.0118	1.0094	1.0110	0.0016
5	1.0100	1.0100	1.0100	0.0000
6	1.0103	1.0096	1.0100	0.0004
7	1.0024	1.0020	1.0023	0.0003
8	1.0100	1.0100	1.0100	0.0000
9	*1.0509*	*1.0572*	*1.0507*	*-0.0065*
10	1.0451	1.0195	1.0383	0.0188
11	1.0820	1.0820	1.0820	0.0000
12	1.0571	1.0516	1.0560	0.0044
13	1.0710	1.0710	1.0710	0.0000
14	1.0423	1.0349	1.0398	0.0049
15	1.0377	1.0274	1.0344	0.0070
16	1.0444	1.0289	1.0402	0.0113
17	1.0399	1.0176	1.0373	0.0197
18	1.0282	1.0121	1.0263	0.0142
19	1.0257	1.0063	1.0238	0.0175
20	1.0297	1.0088	1.0266	0.0178
21	1.0327	1.0082	1.0299	0.0217
22	1.0333	1.0092	1.0302	0.0210
23	1.0272	1.0141	1.0240	0.0099
24	1.0216	1.0049	1.0190	0.0141
25	1.0173	1.0089	1.0149	0.0060
26	0.9997	0.9910	0.9952	0.0042
27	1.0232	1.0199	1.0222	0.0023
28	1.0068	1.0053	1.0063	0.0010
29	1.0034	1.0000	1.0028	0.0028
30	0.9919	0.9885	0.9899	0.0014

Table 4: Loading values of lines

	Line Loading Values (% of nominal in Amperes)				
Between Buses	Normal Operating	Outage	UPFC Outage	Fault	UPFC Fault
1-2	126.7	15.8	66.4	126.2	96.3
1-3	63.7	15.8	63.8	64.4	66.5
2-6	89	46.1	59.6	87.2	87.4
3-4	62	14.7	51.1	62.7	62.1
4-6	81.2	3.3	66.9	70.5	73.6
4-12 (TR)	71.5	62.6	67.8	91.1	69.2
5-7	26.6	135.1	99.3	27.6	29.3
6-9 (TR)	44.5	49.8	44.3	19	40.9
6-10 (TR)	49.5	54.3	47.2	85.7	47.5
9-11	24.2	29.4	22	19.4	22
10-20	29.2	32.3	31.1	18.1	23.3
12-16	47.2	38.5	42.2	88.9	55.9
16-17	23.7	16.6	23	65.2	31.1
18-19	17.3	12.3	14.8	41.9	22.6

The system can exactly restore the bus voltages to normal operating condition values for both cases if there is no line-loading limitation.

Tab. 4 clearly shows that the proposed model not only regulates the busbar voltages, but also has the ability to manage the line loadings maintaining optimal values. The control region reaches its maximum performance on the lines that have transformer units.

5 Discussion

Real-time observation of power systems is important to determine and rapidly intervene when certain conditions exist. This is a vital necessity for a quality energy supplement. This paper focused on the observation of a power system in terms of power flow analysis parameters. The proposed approach is a very simple and quick optimization method based on the Gauss-Seidel algorithm to avoid possible erroneous selection of initial values. The algorithm uses data from the whole system. Therefore, the developed model can manage the entire system. The developed controller has been designed for use in real-time operation. The system performs the regulation by using the whole system data, and this protects the system in the case of possible instability conditions.

The system also has positive effects on line loading values. One of the major problems for power systems is transmission losses; however, when a fault occurs, the UPFC structure can regulate line loadings and reduce line loses.

The proposed method has general design, which means that any number of buses can be integrated for analysis. In addition, it has a portable structure that can be used with a microprocessor-based control circuit, such as FPGA to achieve a fast response. Thus, the proposed method is appropriate for use in actual power systems.

References

Banaei, M. R.; Kami, A. R. (2010): Improvement of dynamical stability using interline power flow controller. *Advances in Electrical and Computer Engineering*, vol. 10, no. 1, pp. 42-49.

Cárdenasa, E. A. Z.; Esquivel, C. R. F. (2011): State estimation of power systems containing facts controllers. *Electric Power Systems Research*, vol. 81, pp. 995-1002.

Christie, R. D. (1993): Power systems test case archive. https://www2.ee.washington.edu /research/pstca/.

Da Costa, V. M.; Martins, N.; Pereira, J. R. L. (1999): Developments in the Newton Raphson power flow formulation based on current injections. *IEEE Transactions on Power Systems*, vol. 14, no. 4, pp. 1320-1326.

Farag, H. E.; El-Saadany, E. F.; El Shatshat, R.; Zidan, A. (2011): A generalized power flow analysis for distribution systems with high penetration of distributed generation. *Electric Power Systems Research*, vol. 81, no. 7, pp. 1499-1506.

Garcia, P. A.; Pereira, J. L. R.; Carneiro, J. S.; Da Costa, V. M.; Martins, N. (2000): Three-phase power flow calculations using the current injection method. *IEEE Transactions on Power Systems*, vol. 15, no. 2, pp. 508-514.

Ghatak, U.; Mukherjee, V. (2017): A fast and efficient load flow technique for unbalanced distribution system. *International Journal of Electrical Power and Energy Systems*, vol. 84, pp. 99-110.

Gyugyi, L.; Schauder, C. D.; Williams, S. L.; Rietman, T. R.; Torgerson, D. R. et al. (1995): The unified power flow controller: A new approach to power transmission control. *IEEE Transactions on Power Delivery*, vol. 10, pp. 1085-1097.

Hingorani N.; Gyugyi G. L. (2000): *Understanding FACTS: Concepts and Technology of Flexible AC Transmission Systems*. IEEE Press, USA.

Kamel, S.; Jurado, F. (2014): Power flow analysis with easy modelling of interline power flow controller. *Electric Power Systems Research*, vol. 108, pp. 234-244.

Kamel, S.; Juradoa, F.; Pecas Lopes, J. A. (2015): Comparison of various UPFC models for power flow control. *Electric Power Systems Research*, vol. 121, pp. 243-251.

Kim, S. H.; Lim, J. U.; Moon, S. I. (2000): Enhancement of power system security level through the power flow control of UPFC. *IEEE PES Summer Meeting*, pp. 38-43.

Morsli, S.; Tayeb, A.; Mouloud, D.; Abdelkader, C. (2012): A robust adaptive fuzzy control of a unified power flow controller. *Turkish Journal of Electrical Engineering & Computer Science*, vol. 20, pp. 87-98.

Pourbagher, R.; Derakhshandeh, S. Y. (2018): A powerful method for solving the power flow problem in the ill-conditioned systems. *International Journal of Electrical Power and Energy Systems*, vol. 94, pp. 88-96.

Powell, L. (2004): *Power System Load Flow Analysis.* McGraw-Hill, New York, USA.

Rajabi-Ghahnavieh, A.; Fotuhi-Firuzabad, M.; Othman, M. (2015): Optimal unified power flow controller application to enhance total transfer capability. *IET Generation, Transmission & Distribution*, vol. 9, no. 4, pp. 358-368.

Shaheen, H. I.; Rashed, G. I.; Cheng, S. J. (2011): Optimal location and parameter setting of UPFC for enhancing power system security based on differential evolution algorithm. *International Journal of Electrical Power and Energy Systems*, vol. 33, no. 1, pp. 94-105.

Shameem, A.; Fadi, M.; Albatsh, S. M.; Hazlie, M. (2014): An approach to improve active power flow capability by using dynamic unified power flow controller. *IEEE Innovative Smart Grid Technologies-Asia*, pp. 249-254.

Shao, W.; Vittal, V. (2006): LP-based OPF for corrective FACTS control to relieve overloads and voltage violations. *IEEE Transactions on Power Systems*, vol. 21, no. 4, pp. 1832-1839.

Shojaeian, S.; Naeeni, E. S.; Dolatshahi, M.; Khani, H. (2014): A PSO-DP based method to determination of the optimal number, location, and size of FACTS devices in power systems. *Advances in Electrical and Computer Engineering*, vol. 14, no. 1, pp. 109-114.

Taher, S. A.; Amooshahi, M. K. (2012): New approach for optimal UPFC placement using hybrid immune algorithm in electric power systems. *International Journal of Electrical Power and Energy Systems*, vol. 43, no. 1, pp. 899-909.

Teng, J. H. (2002): A modified Gauss-Seidel algorithm of three-phase power flow analysis in distribution networks. *International Journal of Electrical Power and Energy Systems*, vol. 24, no. 2, pp. 97-102.

Thiyagarajan, V.; Somasundaram, P. (2017): Modeling and analysis of novel multilevel inverter topology with minimum number of switching components. *Computer Modeling in Engineering & Sciences*, vol. 113, no. 4, pp. 461-473.

Yadav, M.; Soni, A. (2016): Improvement of power flow and voltage stability using unified power flow controller. *International Conference on Electrical, Electronics, and Optimization Techniques*, pp. 4056-4060.

Yuan, Z.; de Haan, S. W. H.; Ferreira, J. B.; Cvoric, D. (2010): A FACTS device: Distributed power-flow controller (DPFC). *IEEE Transactions on Power Electronics*, vol. 25, pp. 2564-2572.

Wang, Y.; Song, X.; Yan, Z.; Yan, Y. (2011): Modeling and simulation studies of unified power flow controller based on power-injected method in PSASP. *Artificial Intelligence, Management Science and Electronic Commerce*, pp. 4076-4079.

Zamora-Cárdenasa, E. A.; Alcaide-Morenob, B. A.; Fuerte-Esquivel, C. R. (2014): State estimation of flexible AC transmission systems considering synchronized phasor measurements. *Electric Power Systems Research*, vol. 106, pp. 120-133.

Zhang, F.; Chen, C. S. (1997): A modified Newton method for radial distribution system power flow analysis. *IEEE Transactions on Power Systems*, vol. 12, no. 1, pp. 389-397.

Zimmerman, R. D.; Murillo-Sanchez, C. E.; Thomas, R. J. (2011): Matpower: Steady-state operations, planning and analysis tools for power systems research and education. *IEEE Transactions on Power Systems*, vol. 26, no. 1, pp. 12-19.